High-speed and energy-efficient non-volatile memristive III-V-on-silicon photonic phase shifter

Zhuoran Fang[1,2*], Bassem Tossoun[1], Antoine Descos[1], Di Liang[1], Xue Huang[1], Geza Kurczveil[1], Arka Majumdar[2,3], Raymond G. Beausoleil[1]
[1]*Hewlett Packard Labs, Milpitas, CA 95035, USA*
[2]*Department of Electrical and Computer Engineering, University of Washington, Seattle, WA 98195, USA*
[3]*Department of Physics, University of Washington, Seattle, WA 98195, USA*
**Email address: rogefzr@uw.edu*

Abstract: We demonstrated a non-volatile III-V-on-silicon photonic phase shifter based on HfO_2 memristor with ~400 fJ switching energy, 100 ns switching speed, and an excellent endurance of over 800 cycles.

1. Introduction

Photonic phase shifter is a fundamental building block of programmable photonic integrated circuits (PICs) [1], traditionally achieved by micro-electro-mechanical systems (MEMS) and thermo-optic effect. The drawbacks of these methods are the volatile nature – a constant substantial power (~mW for thermos-optic effect) or bias (>10V for MEMS) must be applied to maintain the states. It is hence highly desirable to develop non-volatile phase shifters which require zero static power consumption. For examples, non-volatile phase shifters based on phase-change materials (PCMs) [2] are very compact and allow true 'set-and-forget' operation, but they are usually subject to high switching energy (~nJ) and slow switching speed (~µs). Non-volatile ferroelectric phase shifter based on BTO [3] can achieve analog operation and consumes low switching energy, but the electro-optic effect is weak and the switching speed is even slower, requiring a train of pulses with a total duration of 1 ms for switching. Although MEMS is also shown to exhibit non-volatile effect, it requires large driving voltage (>20 V) and the switching time can take up to a few seconds imposed by the slow I-V sweep [4]. Here, we demonstrated a non-volatile phase shifter on the III-V-on-Si heteroegeneous platform enabled by the memristor effect [5,6]. The non-volatility arises from switching the InP-HfO_2-Si memristor between high-resistance-state (HRS) and low-resistance-state (LRS) using a single 100 ns voltage pulse. The phase shifter exhibits a switching energy of ~400 fJ, representing over an order of magnitude reduction compared to the state-of-the-art [2,3], and an excellent endurance of over 800 cycles. Moreover, the III-V-on-Si heterogeneous platform is being adopted by more volume CMOS foundries, enabling a seamless integration between laser sources and the energy efficient programmable PICs.

2. A memristor-based III-V-on-silicon hybrid photonic platform

The non-volatile phase shifter is based on the heterogeneous integration between n-type InP and p-type Si sandwiching a high dielectric constant HfO_2 [7], see Fig. 1a. The 250 nm-tall, 1.2 µm-wide Si waveguide is formed by partially etching to a 100 nm slab on one side and fully etched to the buried oxide (BOX) on the other side. A 150 nm-thick n-InP epitaxial layer is transferred to the silicon layer via standard wafer bonding technique with 9.6 nm-thick HfO_2 as the interface oxide. The HfO_2 acts simultaneously as a gate oxide that forms a metal-oxide-semiconductor (MOS) capacitor with the Si and InP, and a memristor switching layer. Fig. 1b shows the fabricated microring resonator integrated with the phase shifter. In the pristine state, the memristor is in the HRS (Fig. 1c left) and applying a negative bias on the n-InP will cause carrier accumulation at the oxide-semiconductor interfaces, which essentially operates as a MOS capacitor. The effective index of the optical mode in the Si waveguide underneath will therefore be modified by the carrier dispersion effect which in turn leads to a phase shift. On the other hand, if a large enough positive bias is applied on the n-InP terminal, oxygen vacancies start to diffuse inside the oxide layer. At a certain threshold a conduction filament (CF) consisting of the oxygen vacancies is formed, see Fig. 1c middle. Such process is termed 'electroforming' and can be visualized in Fig. 1d green line where the current suddenly increases at around 7.5 V and hits the current compliance enforced by the source meter. The memristor is then switched into the LRS and the MOS capacitive effect is supressed/diminished due to the charge leakage. To return the memristor to HRS (i.e., RESET), a bias with opposite polarity is applied to the n-InP that causes joule heating and the retraction of oxygen vacancies, eventually giving rise to the rupture of the CFs. The operation is revealed by Fig. 1d blue lines where the current rapidly increases to around 2.5 µA at around -2 V before collapsing to near zero. The rupture of the CFs brings the memristor back to the HRS and MOS capacitive effect is restored (Fig. 1c right). The memristor can then be switched to the LRS again by applying a positive bias but at lower voltage, between 5 and 6 V, as shown by the orange lines in Fig. 1d. This is because the CFs do not rupture completely during RESET (Fig. 1c right) and less oxygen vacancies need to be displaced by the field to re-connect the CFs. Fig. 1d shows that such SET and RESET operation is repeated for seven consecutive cycles between HRS and LRS.

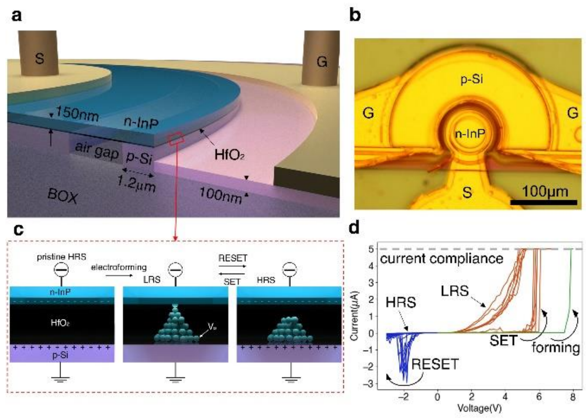

Fig. 1. **a** Schematic of the memristive microring MOS capacitor resonator. **b** Optical micrograph of the microring. **c** Schematics illustrating the working principle of the InP-HfO_2-Si memristor. **d** IV relationship of the electroforming (green), SET (orange), and RESET (blue) operations. The voltage is applied to the n-InP terminal. 'Forming' is short for 'electroforming'.

3. Performances of memristor-based non-volatile phase shifter

Since the memristor can be used to switch the MOS capacitor on and off, it becomes possible to realize non-volatile phase tuning in a microring resonator based on such effect. Fig. 2a shows the reversible switching of the 10 µm radius microring resonator between SET (LRS) and RESET (HRS) states for three consecutive cycles using the device structure shown in Figs. 1a and 1b. Pulses are used instead to switch the memristors, allowing faster operation than the I-V sweep. The shaded regions of the spectra indicate the standard deviation between the three switching cycles, clearly revealing the excellent cycle-to-cycle reproducibility. Note that a constant read voltage of -3 V and a current compliance of 100 nA is applied when taking all the optical measurements here. In the SET state, the MOS capacitor is off. As the memristor is RESET into the HRS, the MOS capacitor is turned on and a blue shift of 0.44 nm is observed, corresponding to a phase shift of 0.088π for a phase shifter length of 47 µm. We further show in Fig. 2b that the phase tuning is indeed non-volatile by monitoring the resonance wavelengths over 1 hour where the two phase-levels remain stable over the time, with only minimal variation due to the drift in optical alignments.

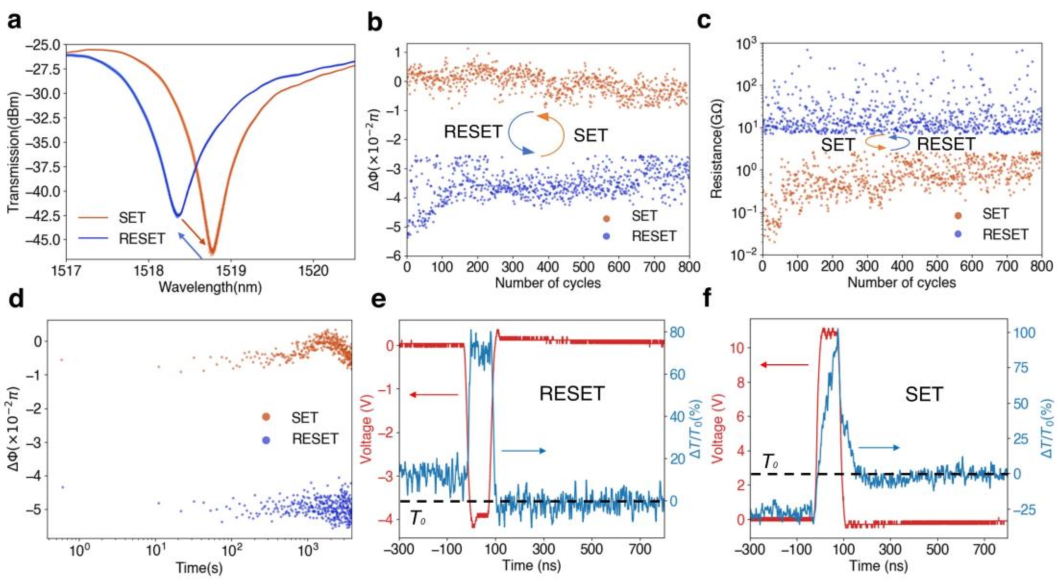

Fig. 2. **a** Reversible switching of microring resonance using memristors. The switching conditions are 7 V for SET and -3 V for RESET both at 200 ns pulse width. **b** Cyclability of the phase shifter for 800 consecutive cycles. The switching conditions are 15 V for SET and -

3 V for RESET, both at 100 ns pulse width. **c** Simultaneous resistance readout of the memristor switching measured at -0.7 V read bias over the 800 cycles. The pulse conditions are the same as in **b**. **d** Time stability test over 1 hour of the SET and RESET phase states. The optical spectrum is measured every 10 seconds to calculate the resonance wavelength. ΔΦ denotes the optical phase shift. Dynamics of **e** RESET and **f** SET operation, together with the voltage pulse that triggers the switching. $\Delta T/T_0$ is defined as $(T-T_0)/T_0$ where T_0 is the average baseline transmission indicated by the black dash line.

Device endurance is a key metric in assessing the durability of the non-volatile phase shifter. Here, we performed over 800 cycles on the phase shifter without significant degradation in the performance, see Fig. 2c. A phase shift of ~0.03π can still be measured after 800 cycles. Meanwhile in the electrical domain, the current is also monitored in each cycle to estimate the resistance. A resistance contrast of 10× is measured across the 800 cycles where both LHS and RHS exhibit a high resistance of >1 GΩ. The good match between the cyclability in optical and electrical domains is a solid proof that the non-volatile phase tuning originates from the memristor switching. Since both states exhibit high resistance, we extract a low switching energy of 1.3 pJ for SET and 400 fJ for RESET by averaging across multiple devices, representing over an order of magnitude reduction in switching energy compared to the state-of-the-art [2,3]. Such low switching energy is an intrinsic advantage of memristor - since the CFs responsible for the switching are only nanometer scale, only minimal current (~µA) and time (100 ns) is required to form and break the filaments.

Lastly, we show that SET and RESET have sub-microsecond optical response time, see Figs. 2e and 2f. Notably, a single 100 ns pulse is enough to trigger both the SET and RESET, compared to microseconds required for PCMs [2] and milliseconds for ferroelectric materials [3]. We estimate an optical response time of ~100 ns for RESET (Fig. 2e) and ~500 ns for SET (Fig. 2f), respectively. The different response time and dynamics are due to distinct effects responsible for SET and RESET. When resetting the memristor, the optical response changes almost simultaneously with the voltage pulse due the rapid carrier accumulation. The fast response is a signature of carrier accumulation effect where >15 GHz-level bandwidth has been measured in MOS capacitor modulator [8]. The non-volatile switching is visualized by a permanent change in optical transmission after the transient effect dies out, indicated by the black dash lines. On the other hand, when setting the memristor, carrier depletion happens first as the bias becomes positive and then carrier injection quickly follows once the CFs form. However, since the MOS capacitor is already in the carrier depleted state at zero bias, further carrier depletion hardly gives any optical change. In fact, the ‘spike’ response observed in Fig. 2f is caused by the slower carrier injection along with thermo-optic effect after the formation of CFs. The change of dynamics from a typical carrier accumulation to a carrier injection response clearly shows that the non-volatile optical switching is caused by the memristor.

4. Conclusion

To summarize, we have demonstrated a non-volatile III-V-on-Si phase shifter with ultra-low switching energy (~400 fJ) and fast speed (~ 100ns). The non-volatile phase shifter also has an excellent endurance of over 800 cycles or 1,600 transitions. The superior performance is made possible by the well-studied electronic memristive effects that have long been explored for non-volatile storage and in-memory computing. The switching lifetime is currently limited by the current overshoot during the SET that switches the memristor into a very low resistance state, which can be addressed by using a MOSFET as the current limiter in the future. Our results show that memristor can be an energy efficient, fast, and reliable technology to realize non-volatile phase tuning in PICs.

5. References

1. W. Bogaerts, D. Pérez, J. Capmany, D. A. B. Miller, J. Poon, D. Englund, F. Morichetti, and A. Melloni, "Programmable photonic circuits," Nature **586**, 207–216 (2020).
2. Z. Fang, R. Chen, J. Zheng, A. I. Khan, K. M. Neilson, S. J. Geiger, D. M. Callahan, M. G. Moebius, A. Saxena, M. E. Chen, C. Rios, J. Hu, E. Pop, and A. Majumdar, "Ultra-low-energy programmable non-volatile silicon photonics based on phase-change materials with graphene heaters," Nat. Nanotechnol. 1–7 (2022).
3. J. Geler-Kremer, F. Eltes, P. Stark, D. Stark, D. Caimi, H. Siegwart, B. Jan Offrein, J. Fompeyrine, and S. Abel, "A ferroelectric multilevel non-volatile photonic phase shifter," Nat. Photon. **16**, 491–497 (2022).
4. P. Edinger, A. Y. Takabayashi, C. Errando–Herranz, U. Khan, C. Antony, G. Talli, P. Verheyen, W. Bogaerts, N. Quack, and K. B. Gylfason, "A Bistable Silicon Photonic Mems Phase Switch For Nonvolatile Photonic Circuits," in *2022 IEEE 35th International Conference on Micro Electro Mechanical Systems Conference (MEMS)* (2022), pp. 995–997.
5. D. B. Strukov, G. S. Snider, D. R. Stewart, and R. S. Williams, "The missing memristor found," Nature **453**, 80–83 (2008).
6. B. Tossoun, X. Sheng, J. P. Strachan, D. Liang, and R. G. Beausoleil, "Hybrid memristor optoelectronic integrated circuits for optical computing," in *Smart Photonic and Optoelectronic Integrated Circuits 2022* (SPIE, 2022), Vol. 12005, pp. 32–36.
7. X. Huang, D. Liang, C. Zhang, G. Kurczveil, X. Li, J. Zhang, M. Fiorentino, and R. Beausoleil, "Heterogeneous MOS microring resonators," in *2017 IEEE Photonics Conference (IPC)* (2017), pp. 121–122.
8. S. Srinivasan, D. Liang, and R. G. Beausoleil, "Heterogeneous SISCAP Microring Modulator for High-Speed Optical Communication," in *2020 European Conference on Optical Communications (ECOC)* (2020), pp. 1–3.